Full-band Ballistic Quantum Transport in Nanostructures using Empirical Pseudopotential

J. Fang*, W. Vandenberghe, and M.V. Fischetti
*The University of Texas at Dallas, 800 W. Campbell Road, Richardson, Texas 75080 USA
e-mail: jxf114930@utdallas.edu

INTRODUCTION

In order to assess the potential performance of nanoscale, low-dimensionality Field Effect Transistors (FETs), we present a method to simulate ballistic quantum transport applying here it to the specific case of silicon Nanowire (Si NW) FETs. The band structure – real and complex – is calculated using empirical pseudopotentials. We employ the supercell method to treat the 2D quantum confinement and the envelope wavefunction approximation to deal with open boundary conditions. Extending work presented before in Ref. [1], we discuss how larger stuctures can now be studied efficiently employing parallelization of the code and sparse matrix solvers.

THEORY

We solve the full-band quantum-transport equation with open boundary conditions employing local empirical pseudopotentials within the envelope function approximation,

$$\sum_G (-\frac{\hbar^2}{2m}\nabla^2\phi^{\mathbf{k}}_{\mathbf{G}}(\mathbf{r}) - \frac{\mathrm{i}\hbar^2}{m}\mathbf{G}\cdot\nabla\phi^{\mathbf{k}}_{\mathbf{G}}(\mathbf{r}) + \frac{\hbar^2|\mathbf{G}|^2}{2m}\phi^{\mathbf{k}}_{\mathbf{G}}(\mathbf{r}) + V^{\mathrm{ext}}(\mathbf{r})\phi^{\mathbf{k}}_{\mathbf{G}}(\mathbf{r}))\delta_{\mathbf{G}\mathbf{G}'} + \sum_G V_{\mathbf{G}\mathbf{G}'}\phi^{\mathbf{k}}_{\mathbf{G}}(\mathbf{r}) = E_{\mathbf{k}}\phi^{\mathbf{k}}_{\mathbf{G}'}(\mathbf{r}). \quad (1)$$

The complex band-structure of the contacts (here assumed to be an extension of the Si NW) must be employed to determine the proper injecting/absorbing boundary conditions, as described in Ref. [1]. Note that in the equation above the dependence on the 'transverse' wavevectors (k_x, k_y) disappears since we consider a one-dimensional nanowire in vacuum. We then solve self-consistently the one-dimensional Poisson equation

$$\nabla^2 V(z) = -\frac{e(N_d(z) - n(z))}{\epsilon} = -\frac{\rho}{\epsilon} \quad (2)$$

where the electron density is obtained by integrating the wavefunctions over the cross section of the NW,

$$n(z) = \sum_\nu \int_{E_c^\nu}^{\infty} \sum_{k_z} D^\nu(k_z)|\psi^\nu_{\mathbf{k}}(z)|^2 F^\nu(E_f^\nu)dE \quad (3)$$

where ν is the index labeling the (source or drain) contacts, $D^\nu(k_z)$ is the density of states, and $F^\nu(E_f^\nu)$ the Fermi-Dirac distribution in the contacts. Finally, the current density is calculated using

$$j_{\mathbf{k}}(z) = \frac{i\hbar}{2m}\sum_{\mathbf{G}} \phi^\star_{\mathbf{G}}(z)(\frac{\mathrm{d}\phi_{\mathbf{G}}(z)}{\mathrm{d}z} + \mathrm{i}G_z\phi_{\mathbf{G}}(z)). \quad (4)$$

RESULTS AND CONCLUSION

We study an n^+in^+ quantum wire of dimensions 0.384 nm×0.384 nm×6.516 nm (*i.e.*, one-cell cross-section, 12-cell long). Figure 1 shows the band structure with a higher cut-off energy than that used in Ref. [1]. The increased computational demands are alleviated by parallelizing our code and using sparse matrix solver. To verify the numerical stability and as a first test of the formalism, we show the current along the transport direction in Fig. 2. Figures 3 and 4 show the potential and charge density profiles, respectively. Finally, we obtain the I_D versus V_{DS} characteristics of the device in Fig. 5, showing Ohmic behavior at low biases. Results for gated armchair-edge graphene nanoribbons (aGNRs) and narrow transition-metal dichalcogenides (TMDs) channels will also be presented.

ACKNOWLEDGMENT

This work has been supported in part by Samsung Electronics Ltd. and by the Nanoelectronics Research Initiative's (NRI's) Southwest Academy of Nanoelectronics (SWAN). Discussions with professor William Frensley are also acknowledged.

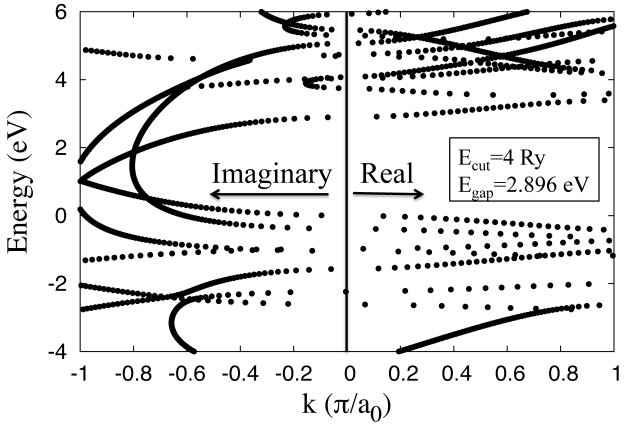

Fig. 1: Complex band structure of silicon nanowire. The imaginary part of the wavevector is shown on the left, the real part on the right.

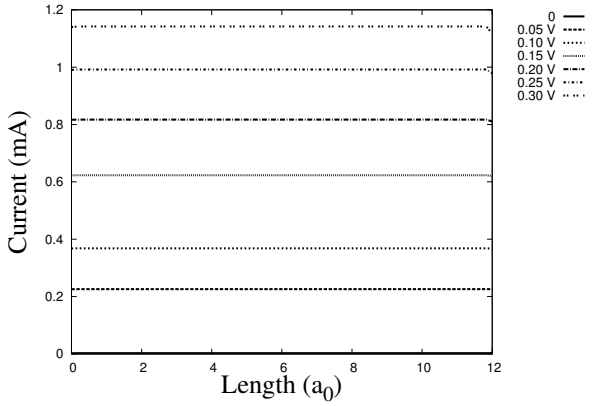

Fig. 2: Current density along the device for different bias conditions. Note the satisfactory current conservation.

REFERENCES

[1] **M. V. Fischetti**, Bo Fu, S. Narayanan, and J. Kim, *S*emiclassical and Quantum Electronic Transport in Nanometer-Scale Structures: Empirical Pseudopotential Band Structure, Monte Carlo Simulations and Pauli Master Equation, in *"Nano-Electronic Devices: Semiclassical and Quantum Transport Modeling"*, D. Vasileska and Stephen M. Goodnick Eds. (Springer, New York, 2011), pp. 183-247; B. Fu and M.V. Fishcetti, *Open Boundary-Condition Ballistic Quantum Transport using Empirical Pseudopotentials*, IWCE16 (2013).

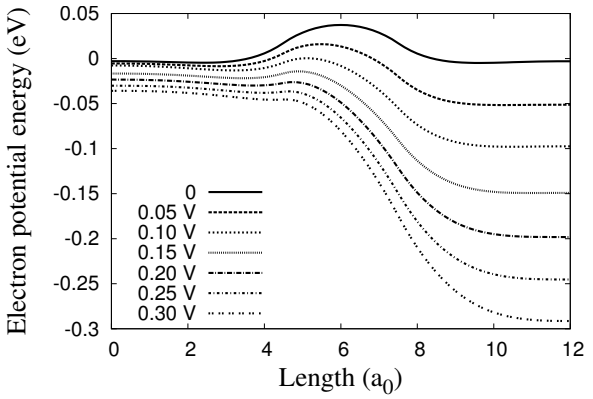

Fig. 3: Electron potential energy along the device for different source/drain bias conditions.

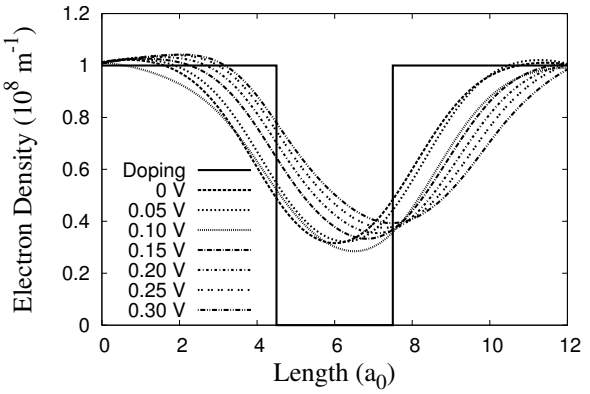

Fig. 4: Initial doping profile (solid) of the device and electron density distribution (dashed) in different regions of the device under different bias conditions.

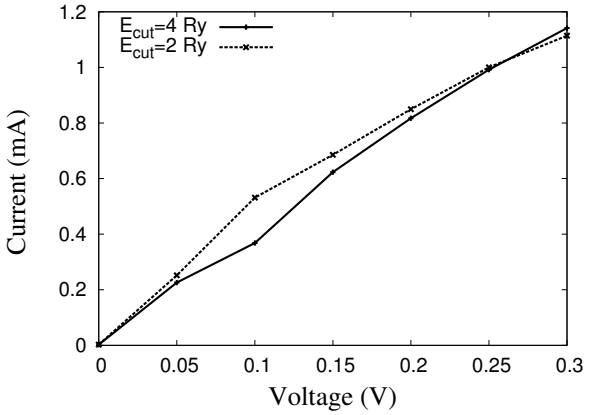

Fig. 5: I_D-V_{DS} Characteristics of the device under operation with different cut-off energies. Even using a low energy cut-off of 2 Ry for faster calculations, the current is reasonably accurate, as compared to results obtained employing higher cut-off energies.